Hypercoagulable State in COVID-19 and Diabetes: Cerebral Vasospasm, Intracardiac Clot, and Pulmonary Embolism

Philip Chidi Njemanze, Chinenye U. Mgbenu, Chinwendu C. Darlington, Clara C. Ofoegbu, Nneoma E. Ukeje, Ijeoma A. Ohaegbulem, Esther C. Nneke, Joy E. Onuchukwu, Chidimma O. Ukaegbu, Marvis Amuchie, Clinton O. Mezu, Juliet Chizoma Anaele, Ogechi Uzoma, Chinonso Mbara, Anthonia Amadi, Benedicta Iwuagwu

Chidicon Medical Center, Institute of Non-Invasive Imaging for Parasitology, International Institutes of Advanced Research and Training, Owerri, Imo State, Nigeria

Abstract

Background: Hypercoagulable state in the form of venous and arterial thromboembolism, associated with poor prognosis, could be a severe sequel of COVID-19 infections. We present representative cases that show hypercoagulable state in COVID-19 and the negative effects of diabetes and age on outcomes of anticoagulation therapy. Our aim is to understand the role of predisposing factors for the successful use of anticoagulants. **Methods:** We applied clinical history, examination, laboratory tests, noninvasive ultrasound imaging, and computer-assisted tomography to characterize hypercoagulable state in patients with COVID-19. **Results:** One patient (83 years) was diabetic of the elderly group (>64 years), who developed sepsis-induced coagulopathy (SIC), cerebral arterial vasospasm, intracardiac clots, coronary ischemia, and pulmonary embolism with fatal outcome despite the use of anticoagulation. The second patient (60 years) was diabetic of the middle-age group (48–63 years), who developed SIC, cerebral arterial vasospasm, intracardiac clots, and coronary ischemia and had good outcome with the use of anticoagulation. The third case was a patient (22 years) without diabetes of the youth group (15–47 years) who developed cardiomyopathy, heart valve vegetations, and cerebral arterial vasospasm, received anticoagulation, and had good outcome. The difference in outcome with the application of anticoagulation with lower molecular weight heparin could be related to the greater burden of disease including diabetes, age, and chronic obstructive pulmonary disease. **Conclusion:** Noninvasive ultrasound imaging modalities in combinations with computed axial tomography scans provided insightful characterization of the hypercoagulable state of COVID-19 infection, which helped guide therapeutic intervention.

Keywords: Coagulation, COVID-19, diabetes, pulmonary embolism, thrombus, vasospasm

Introduction

Hypercoagulable state in the form of venous and arterial thromboembolism, associated with poor prognosis, could be a severe sequel of COVID-19 infections.[1-4]

Several hypotheses have been proposed which include a severely heightened inflammatory response that leads to thromboinflammation, through mechanisms such as cytokine storm, complement activation, and endotheliitis.[2-8] Others have suggested direct viral activation of the coagulation cascade.[9] To remedy coagulopathy, investigators have applied lower molecular weight heparin (LMWH) at prophylactic doses in the management of COVID-19 patients.[10] Patients with sepsis-induced coagulopathy (SIC) score of greater than 3 had decreased 28-day mortality as did the patients with D-dimer greater than 6 times the upper limit of normal. However, thrombotic complications have been reported despite the use of prophylactic anticoagulation with LMWH in patients with COVID-19 pneumonia.[5] It was concluded that hypercoagulable state exists in patients with severe COVID-19 infection, and there is a high risk of significant thromboembolism despite the use of prophylactic and therapeutic doses of anticoagulation.[6] The hypercoagulable state in COVID-19 is emerging as a major pathological occurrence with serious consequences for mortality and

Access this article online

Quick Response Code:

Website: www.njgp.org

DOI: 10.4103/njgp.njgp_3_22

Address for correspondence: Academician. Dr. Philip Chidi Njemanze, Chidicon Medical Center, Institute of Non-Invasive Imaging for Parasitology, International Institutes of Advanced Research and Training, Owerri, Imo State, Nigeria.
E-mail: philip.njemanze@chidicon.com

How to cite this article: Njemanze PC, Mgbenu CU, Darlington CC, Ofoegbu CC, Ukeje NE, Ohaegbulem IA, *et al.* Hypercoagulable state in COVID-19 and diabetes: Cerebral vasospasm, intracardiac clot, and pulmonary embolism. Niger J Gen Pract 2022;20:6-13.

Submitted: 24-Feb-2022 **Accepted:** 10-May-2022
Published: 12-Nov-2022

morbidity. The most common thrombotic complication of COVID-19 pneumonia is pulmonary embolism (PE).[6] Myocardial infarction was not a frequently (1.1%) reported thrombotic complication in COVID-19.[11,12] The primary site of thrombotic microangiopathy (TMA) was in the lungs.[13-15]

Diabetes is one of the major predisposing conditions for complications in COVID-19 infection. According to the CDC's 2017 National Diabetes Statistics Report, there were around 1.5 million new total diabetes cases among adults in 2015. In 2015, adults aged 45–64 years were the most diagnosed age group for diabetes. Diabetes is similar to proinflammatory state that is associated with a hypercoagulable state. Diabetic patients with COVID-19 are at increased risk of thromboembolic events and death.[16] In COVID-19, there is proinflammatory response and cytokine storm which precipitates hypercoagulation in some patients. Patients with diabetes are more predisposed to proinflammatory response and hence at greater risk of thromboembolic events in COVID-19. In diabetes, hyperglycemia promotes coagulation, as well as hyperinsulinemia, which inhibits fibrinolytic activity.[17]

We present representative cases that show hypercoagulable state in COVID-19 and the negative effects of diabetes and age on the outcome of anticoagulation therapy. We hope to understand the role of predisposing factors for the successful use of anticoagulants. One patient (83 years) was diabetic of the elderly group (>64 years), who developed SIC, cerebral arterial vasospasm, intracardiac clots, coronary ischemia, and PE with fatal outcomes despite the use of anticoagulation. The second patient (60 years) was diabetic of the middle-age group (48–63 years), who developed SIC, cerebral arterial vasospasm, intracardiac clots, and coronary ischemia and had good outcome with the use of anticoagulation. The third case was a patient (22 years) without diabetes of the youth group (15–47 years) who developed cardiomyopathy, heart valve vegetations, and cerebral arterial vasospasm, received anticoagulation, and had a good outcome. The difference in outcome with application of anticoagulation with LMWH could be related to the greater burden of disease including diabetes, age, and chronic obstructive pulmonary disease (COPD).

Methods

We demonstrate three representative cases of COVID-19 patients in hypercoagulable state. The COVID-19 infection was diagnosed based on the clinical presentation as defined in the National Interim Guidelines for Clinical Management of COVID-19 version 3, June 2020, issued by the Nigeria Centre for Disease Control (NCDC). Severe cases were defined as the presence of severe conditions: difficulty in breathing, crackles in lungs, reduced/decreased breath sounds, dullness in percussion, increased or decreased vocal resonance, and presence of comorbid conditions such as diabetes, asthma, hypertension, and COPD. Laboratory tests using antibody tests (Standard™ Q COVID-19 Ag test, SD Biosensor, Republic of Korea) were positive for COVID-19 in all patients. Laboratory tests including blood sample analysis and biochemistry were conducted. Twelve-lead electrocardiography (ECG) was recorded. Ultrasonographic examination with two-dimensional echocardiography (2D-Echo) was performed using a wide-angle, phased array multifrequency S4 transducer of the scanner from Philips Agilent HP M2424A Sonos 5500 (Hewlett-Packard, Andover, Massachusetts, USA). 2D-Echo images were obtained using the techniques recommended by the American Society of Echocardiography guidelines.[18] The 2D-Echo images in the parasternal long-axis, short-axis, apical two-chamber, and four-chamber views were obtained. 2D-Echo images identified thrombus as a distinct mass of echoes in the left ventricular cavity that was contiguous with the endocardium in an area of abnormal wall motion of hypokinesia or dyskinesia present throughout the cardiac cycle in at least two different echocardiographic views.

Transcranial Doppler (TCD) ultrasound was performed with the 1.8 MHz Doppler mode of the multifrequency S4 transducer of the same ultrasound equipment. We measured the cerebral blood flow velocities including peak systolic velocity (PSV), mean flow velocity (MFV), end-diastolic velocity (EDV), and pulsatility index (PI) in the major basal cerebral arteries of the circle of Willis, including the right and left anterior cerebral artery (RACA, LACA), right and left middle cerebral artery (RMCA, LMCA), right and left internal carotid artery (RICA, LICA), right and left posterior cerebral artery (RPCA, LPCA), and basilar artery (BA) in the supine horizontal position. TCD provides a rapid, non-invasive, real-time measurement of cerebral blood flow velocities in the major intracranial arteries.[19,20] The examinations were performed through the temporal acoustic windows on the left and right temporal bones for ipsilateral insonation of the arteries of the circle of Willis on the left and right sides, respectively. Duplex carotid ultrasound was used to examine the extracranial arteries with 7.5 MHz mode of the same S4 probe. Carotid Duplex ultrasound with B-mode images and Doppler flow velocities were obtained in the right and left common carotid artery, RICA, LICA, and right and left external carotid artery, respectively. We calculated the Lindegaard ratio (LR) which is the ratio of the MFVs in the MCA and the ipsilateral extracranial ICA. Its primary utility is, in the context of increased MCA velocities after subarachnoid hemorrhage, to confirm the presence of vasospasm. However, it was applied to other arterial branches of the anterior circulation of the ipsilateral ICA.[20] LR above 3 supports the diagnosis of vasospasm. Computed axial tomography (CAT) was obtained if indicated by the presence of severe focal neurologic symptoms. Brain and skull scans were obtained in coronal, axial, and sagittal planes in pre- and post-contrast phase. Treatment regimen followed the NCDC National Interim Guidelines for Clinical Management of COVID-19 version 3, June 2020, in addition to the use of anticoagulation at prophylactic or therapeutic doses if indicated. Informed consent obtained and the institutional ethics review approved the study.

Results

Case 1 presentation

An 83-year-old Nigerian male patient presented with severe general weakness, anorexia, high fever (40°C), shortness of breath, cough with productive sputum, loss of concentration, loss of memory, prosopagnosia, and pedal edema. The present illness started 10 days before admission with weakness and loss of appetite. He had a history of long-standing diabetes, hypertension, and COPD. The blood pressure was 104/60 mmHg and the heart rate was 88 bpm. The oxygen saturation was 68%. The body mass index was 21. CAT scan examination revealed multiple areas of cerebral infarction predominantly in the right cerebral hemisphere. The initial blood sample analysis revealed hematocrit (HCT) of 42%, hemoglobin (Hb) of 14 g/dL, white blood cell count (WBC) of 7000/mm^3, erythrocyte sedimentation rate (ESR) of 88 mm/h, clotting time (CT) of 5 min, platelet count of 200,000/mm^3, and prothrombin time (PTT) of 20 s. Malaria parasites were seen in the blood. There was electrolyte imbalance showing hypernatremia (sodium 160 mEq/L), hyperkalemia (potassium 6.0 mEq/L), hypermagnesemia (magnesium 4.2 mg/dL), hypocalcemia (calcium 2.2 mg/dL), and hypochloremia (chloride 94 mEq/L). The uric acid (6.2 mg/dL) level was normal. The urea (62 mg/dL) level was raised. He was of blood group O, Rhesus positive. Serology tests including hepatitis B antigen, hepatitis C antigen, and HIV test were negative. The liver function enzymes such as aspartate aminotransferase (AST, 17 IU/L) and alanine aminotransferase (ALT, 9 IU/L) were within normal range. There was hyperbilirubinemia; the total bilirubin (1.5 mg/dL) and conjugated bilirubin (1.2 mg/dL) were raised. Fasting blood sugar (FBS, 309 mg/dL) was very high. The hemoglobin A1C (HbAIC 7.6%) was raised, even with strict compliance to antidiabetic drug therapy. Lipid profile: total cholesterol (TCHOL 159.6 mg/dL), low-density lipoprotein (LDL 78 mg/dL), high-density lipoprotein (HDL 62 mg/dL), triglyceride (TG 98 mg/dL), and very LDL (VLDL 19.6 mg/dL) was within normal range. Urinalysis revealed urinary tract infection (WBCs 3–4/HPF), bacteria (cocci) were present, and epithelial cells were numerous.

A repeat blood sample analysis done 5 days later showed HCT of 30.2%, Hb of 10.4 g/dL, WBC of 11,000/mm^3, ESR of 60 mm/h, CT of 8 min, platelet count of 140,000/mm^3, and PTT of 22 s. The electrolytes were within normal range; however, there were a precipitous rise in urea (175 mg/dL), hyperbilirubinemia, and slightly raised liver enzyme (AST 52 IU/L). There was rapidly developing anemia and DIC with platelet consumption induced by SIC and renal impairment.

The initial ECG revealed a ventricular heart rate of (VR 83 bpm) and atrial rate (AR 83 bpm). There was inverted T-wave in leads I, II and deep symmetrical T-wave inversion in leads V3, V4, V5, and V6, respectively, suggestive of postcardiac ischemia [Figure 1].

Figure 2a and b shows the 2D-Echo in long-axis view demonstrating a clot measuring a size of 1.19 cm × 1.34 cm on the apical septal wall [Figure 2a, within small crosses] and in cross-sectional view, shows a clot of size 1.17 cm × 0.99 cm on the apical septal wall [Figure 2b, within small crosses]. The end-diastolic volume was 33.1 mL, and the posterior wall thickness was 1.26 cm; the systolic volume was 16.1 mL, and the posterior wall thickness was 1.4 cm. There was dyskinetic wall motion abnormality of the apical septal wall. The ejection fraction was reduced to 51.4%.

Figure 2a-f shows intracardiac clots on 2D-Echo in long-axis [Figure 2a] and short-axis views [Figure 2b]; CAT revealed multiple irregular hypodense areas in the right prefrontal cortex [Figure 2c, small arrows]. The latter corresponds to the area of supply of the RACA. TCD [Figure 2d] revealed vasospastic cerebral blood flow velocities in the RACA: PSV - 163 cm/s, MFV - 107 cm/s, EDV - 68.1 cm/s, PI - 0.88, and LR - 3.3. CT revealed hypodense area in the right temperoparietal region [Figure 2e, small arrow] along a vasospastic RPCA. TCD revealed highly vasospastic flow velocities in the RPCA: PSV - 257 cm/s, MFV - 160 cm/s, EDV 95 cm/s, and PI - 1.01 [Figure 2f, small arrow]. There were normal flow velocities in the LPCA and BA regions, not seen in the CAT scan volume [Figure 2e, small arrow head].

The patient was managed for acute respiratory distress syndrome and septic shock. Magnetic resonance imaging studies undertaken before admission suggested that the patient had developed signs of PE. The patient received anticoagulation treatment at prophylactic doses (LMWH – enoxaparin 40 mg s.c. once daily). Unfortunately, he passed on shortly thereafter.

Case 2 presentation

A 60-year-old Nigerian male presented with insomnia, severe general weakness, anorexia, restlessness, chills but no fever, shortness of breath, and cough with productive sputum. The present illness started 2 weeks ago with cough, sore throat, and very high level of FBS. He had a history of long-standing diabetes and hypertension. The blood pressure was 117/72 mmHg and the heart rate was 103 bpm. The patient was in severe hypoxemia with oxygen saturation at 33%. The body mass index was 32.7. Hematological analysis revealed HCT of 40%, Hb of 13.3 g/dL, WBC of 10,200/mm^3, ESR of 80 mm/h, CT of 6 min, platelet count of 200,000/mm^3, and PTT of 23 s. Malarial parasites were seen in the blood. The electrolyte was normal (sodium - 155 mEq/L; potassium - 4.2 mEq/L; and chloride 98 mEq/L). However, there was slight hypercalcemia (calcium 10.7 mg/dL). The urea (39 mg/dL) was normal. He was of blood group O Rhesus positive. Serology tests including hepatitis B antigen, hepatitis C antigen, and HIV test were negative. The liver function enzymes (AST 10 IU/L and ALT 9 IU/L) were within normal range. The total bilirubin (0.2 mg/dL) and conjugated bilirubin (0.2 mg/dL) were normal. FBS (235 mg/dL) was very high. The HbAIC (9.1%) was raised with a history of poor compliance with antidiabetic drug therapy. Lipid profile: TCHOL - 166 mg/dL, LDL - 92 mg/dL, and HDL - 28 mg/dL was normal,

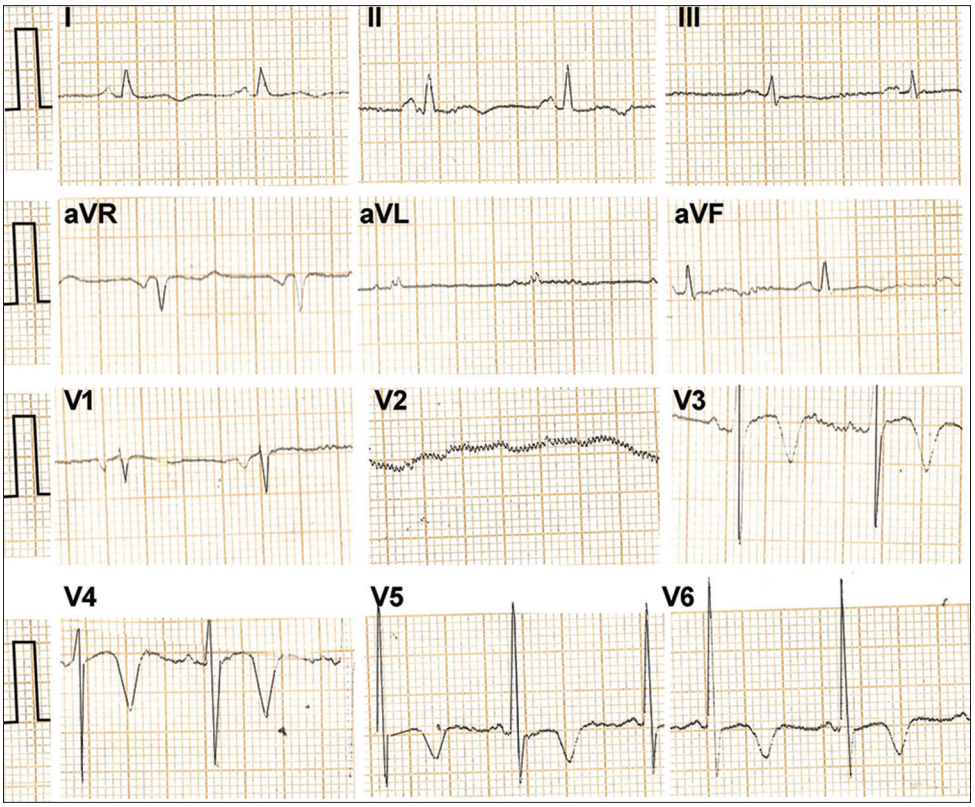

Figure 1: Top panel shows inverted T-waves in the leads I, II, V3, V4, V5, and V6

but there was hypertriglyceridemia (TG - 231 mg/dL and VLDL - 46 mg/dL). Urinalysis revealed urinary tract infection (WBCs 1–2/HPF); epithelial and yeast cells were present. There were glucosuria, hematuria, and proteinuria.

Subsequently, he appeared pale and the blood analysis revealed severe anemia (HCT 25% and Hb 8.3 g/dL). The WBC (7200/mm^3) was normal, but ESR (91 mm/h) was raised. The CT (11 min), platelet count (151,000/mm^3), and PTT (37 s) were within normal range. Two days later, the platelet count depleted further to 100,000/mm^3 with a rise in ESR (95 mm/h), suggestive of SIC and DIC.

The initial ECG revealed paroxysmal atrial fibrillation, ventricular rate 100 bpm, S-T depression, right bundle branch block, and abnormally low R wave amplitude extending from the right to the left precordial leads, indicating the presence of left ventricular hypertrophy.

The 2D-Echo [Figure 3a] in short-axis view showed a clot of size 1.85 cm × 2.05 cm on the apical septal wall [Figure 3a, small white arrow] and in long-axis view showed a clot of size 2.59 cm × 1.43 cm on the apical septal wall [Figure 3b, small white arrow]. There was increased end-diastolic volume (66.4 mL), posterior wall thickness (1.59 cm), systolic volume (41.2 mL), and posterior wall thickness (1.88 cm). There was dyskinetic wall motion abnormality of the apical septal wall. The ejection fraction was reduced to 41.2%. The intracardiac clots generated cardiogenic microemboli which were discharged into the brain circulation. The posttreatment 2D-Echo in short-axis [Figure 3c, white arrow head] and long-axis view [Figure 3d, white arrow head] did not show any clots.

TCD [Figure 3e] showed vasospasm in LICA: PSV - 258 cm/s, MFV - 190 cm/s, EDV - 129 cm/s, PI - 0.679, and LR - 3.1. There was widespread microembolization in other arteries of the anterior circulation including the LACA: PSV - 170 cm/s, MFV - 107 cm/s, EDV - 61 cm/s, and PI - 1.02; LMCA: PSV - 159 cm/s, MFV - 97.6 cm/s, EDV - 61 cm/s, and PI - 1.0. However, flow velocities were normal in the posterior circulation [Figure 3f], BA: PSV - 123 cm/s, MFV - 73 cm/s, EDV - 41.7 cm/s, and PI - 1.11. The patient was successfully declotted using prophylactic dose of anticoagulation (LMWH – enoxaparin 40 mg s.c. daily) over a 10-day duration. Blood transfusion was initiated to treat anemia. The patient's condition improved significantly, and he remained free of any symptoms with SaO_2 >95%. The patient on follow-up visits remained symptom-free with blood tests unremarkable.

Case 3 presentation

A 22-year-old Nigerian male presented with fainting spells with complete loss of consciousness and only resuscitated with oxygen therapy. He had headache, amnesia, anxiety, nervousness, poor vision, photophobia, insomnia, depression, fever, chest pain, severe general weakness, shortness of breath, choking, gasping for air, and cough with productive yellow sputum. The present illness started 2 days before admission with fainting spells and general weakness. The

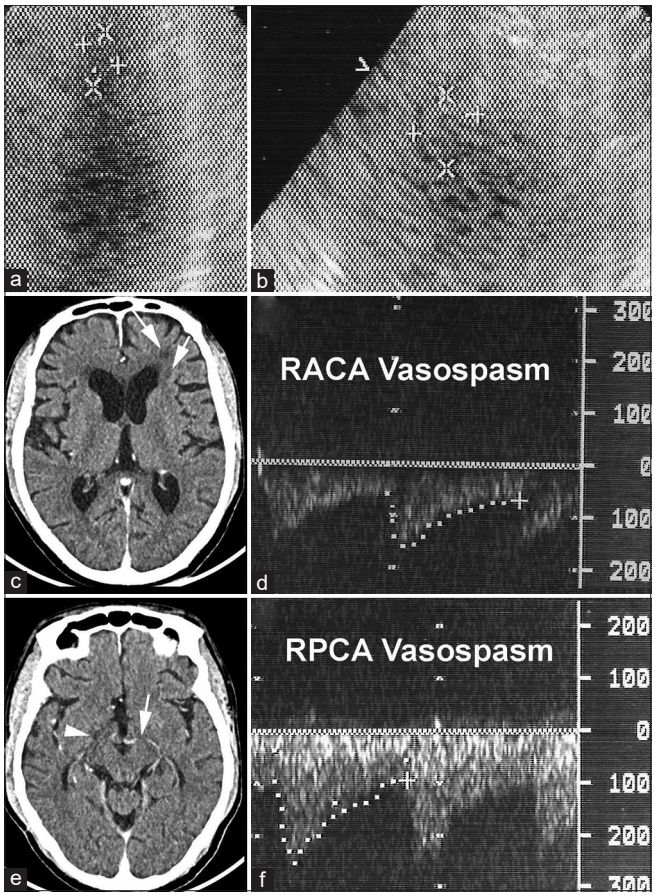

Figure 2: (a-f) Intracardiac clots on two-dimensional echocardiography in the long-axis (a) and short-axis views (b); computed axial tomography scan demonstrates multiple irregular hypodense areas in the right prefrontal cortex (c, small arrows); transcranial Doppler reveals vasospasm in the RACA (d); computed axial tomography scan also shows hypodense area in the right temperoparietal region along the vasospastic segment of the RPCA (e, small arrow), but the LPCA was not within the scan slice (e, arrow head). (f) RACA: Right anterior cerebral artery, RPCA: Right posterior cerebral artery

blood pressure was 112/59 mmHg and the heart rate was 71 bpm. The patient was on oxygen therapy on admission and the saturation was 97%. The body mass index was 25. Hematological analysis revealed HCT of 44.7%, Hb of 14.9 g/dL, WBC of 4000/mm^3, ESR of 10 mm/h, CT of 7 min, platelet count of 130,000/mm^3, and PTT of 25 s. No malarial parasites were seen in the blood. He was of blood group O, Rhesus positive. Lipid profile: TCHOL - 99 mg/dL, LDL - 38 mg/dL, HDL - 43 mg/dL, TG - 90 mg/dL, and VLDL 18 mg/dL was normal. Urinalysis revealed urinary tract infection showing WBCs at 2–3/HPF, cocci, bilirubinuria, and epithelial cells. The initial ECG revealed bradycardia with VR of 55 bpm. There was paroxysmal atrial fibrillation with AR of 500 bpm [Figure 4, V2 and V5 arrow heads]. There was T-wave inversion due to myocardial ischemia in contiguous leads of the inferior wall (leads II, III, and aVF).

The pretreatment 2D-Echo in the short-axis view [Figure 5a] and long-axis view [Figure 5b] showed dilated ventricular dimensions, suggestive of dilated cardiomyopathy. The end-diastolic volume was 129 mL, and the diastolic posterior wall thickness was 1.47 cm; the systolic volume was 44.3 mL, and the systolic posterior wall thickness was 1.62 cm. There was normokinetic wall motion. The ejection fraction was 66.4%. There were no intracardiac clots, but there was thickening of the mitral valve [Figure 5b, small arrow head]. The M-mode [Figure 5c, arrow and arrow head] showed aortic valve vegetations. The patient was successfully declotted with prophylactic dose of anticoagulant (LMWH – enoxaparin 40 mg s.c. daily) over a 10-day duration. The posttreatment 2D-Echo revealed reduced ventricular dimensions, and the end-diastolic volume was 71.7 mL, a reduction of 44.4% suggesting a gradual resolution of the cardiomyopathy. The aortic and mitral valves were of normal thickness. The microemboli from the valvular vegetations were discharged into the cerebral circulation. TCD [Figure 5d] showed significant vasospasm in RMCA (PSV - 211 cm/s, MFV - 129 cm/s, EDV - 96 cm/s, and PI - 0.888). The flow velocities were raised in the other arteries of the anterior circulation, suggesting the wide spread cardiogenic microembolization of the anterior cerebral circulation: LICA – PSV - 176 cm/s, MFV - 101 cm/s, EDV - 80.8 cm/s, and PI - 0.943; LMCA – PSV - 150 cm/s, MFV - 95.6 cm/s, EDV - 73.8 cm/s, and PI - 0.797 [Figure 5e].

Discussion

In the present work, imaging studies demonstrated clots in the cardiac cavities and microemboli-induced cerebral vasospasm in cerebral arteries. The application of prophylactic doses of anticoagulation prevented thrombotic events in two patients, but not in the elderly diabetic patient. There is a need to clearly define the regimen for anticoagulation in elderly diabetics. The clinical presentation in the patients suggests that the hypercoagulability of SARS-CoV-2 involves a unique mechanism of thrombo-inflammation triggered by viral infection, originating in the pulmonary vasculature. The application of imaging modalities allowed a better understanding of the pathophysiology for a successful deployment of the anticoagulation treatment. However, the adequate treatment dose for anticoagulation in the elderly diabetics remains to be determined. Obviously, the comorbid condition of diabetes and COPD and the effects of age put the patient at risk for worse outcomes, despite the use of anticoagulation. The hypercoagulable state is a major complication that determines mortality and morbidity in COVID-19 patients.[4] Recently, we reported similar hypercoagulable state in Lassa fever, suggesting that these viral infections may cause derangement in the hemostatic pathways.

Furthermore, the imaging characterization of the lesions should be used alongside biomarkers of thrombosis in severe illness to guide clinicians on early interventional strategies and to monitor effectiveness of the treatment.

The development of therapeutic strategies for the management of coagulopathy associated with COVID-19 should evolve

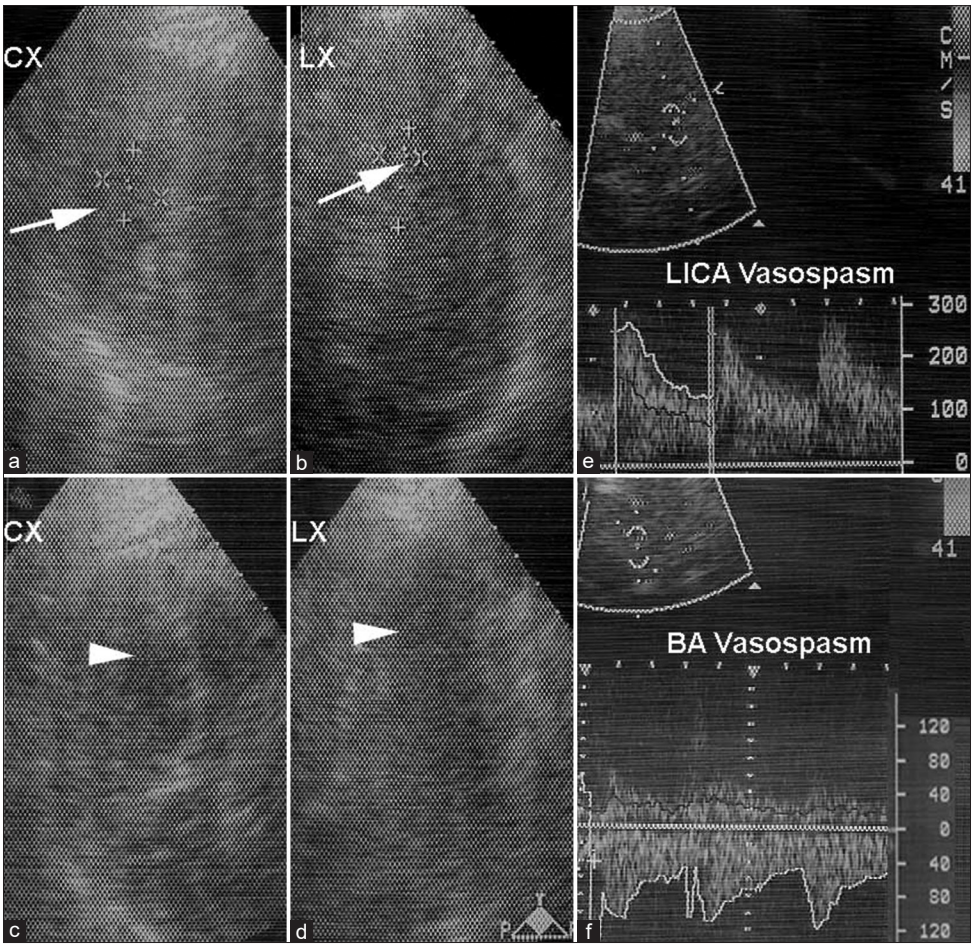

Figure 3: (a-f) shows clot in pretreatment two-dimensional echocardiography short-axis view (a, small white arrow) and in long-axis view (b, small white arrow). The posttreatment two-dimensional echocardiography in short-axis (c, white arrowhead) and long-axis view (d, white arrowhead) did not show any clots. Pretreatment transcranial Doppler showed vasospasm in LICA (e) and BA (f) due to cerebral microembilization. LICA: Left internal carotid artery, BA: Basilar artery

with application of imaging modalities alongside biomarkers. Multicenter studies of COVID-19 patients in different age groups would be needed to prepare guidelines for the management of hypercoagulable state based on what is known about the pathophysiology of thromboinflammation. Although we chose to apply prophylactic dose, there were options for use of intermediate or therapeutic doses of anticoagulation. However, there is the risk of life-threatening bleeding in patients with increasing dose of anticoagulation. While some have demonstrated the beneficial effect of anticoagulation with LMWH in patients with SIC,[10] others have reported incidence of thrombotic complications despite the use of prophylactic anticoagulation with LMWH.[5] There may be need for higher therapeutic dose for elderly diabetic patients, especially if there are no risks of bleeding.[6]

In the elderly diabetic (Case 1), the use of anticoagulation may not be sufficient to prevent pulmonary embolic complications due to comorbid condition of COPD. On-going studies need to examine the pathophysiologic differences in COVID-19–induced coagulopathy in the elderly diabetic patients. Hypercoagulation has been reported in severe COVID-19 patients[21,22] with fatal cases presenting diffuse microvascular thrombosis, as a result of thrombogenic microangiopathy.[23] In type 2 diabetes, the hypercoagulable state also is enhanced by the imbalance between coagulation and fibrinolysis, which in turn enhances clotting factor levels and relative fibrinolytic system stoppage.[24] During the inflammatory cytokine storm, the D-dimer rises geometrically as a result of activation of plasmin during the early stage.[25] This sets off a chain of reactions, as inflammation goes on in hypoxia-induced molecules, which can trigger direct thrombin and activate monocyte macrophages. The latter can also emit tissue factors in masses and open the pathway of exogenous coagulation that results in a general state of hypercoagulability.

Ongoing clinical trials suggest that, all patients with COVID-19 who are started on empiric therapeutic anticoagulation for presumed or documented PE should be given a minimum course of 3 months of the therapeutic regimen (provided the patient tolerates treatment without serious bleeding). Furthermore, they suggest that thrombus resolution can occur within a few days of effective anticoagulation, so negative results from delayed testing should not be interpreted as implying

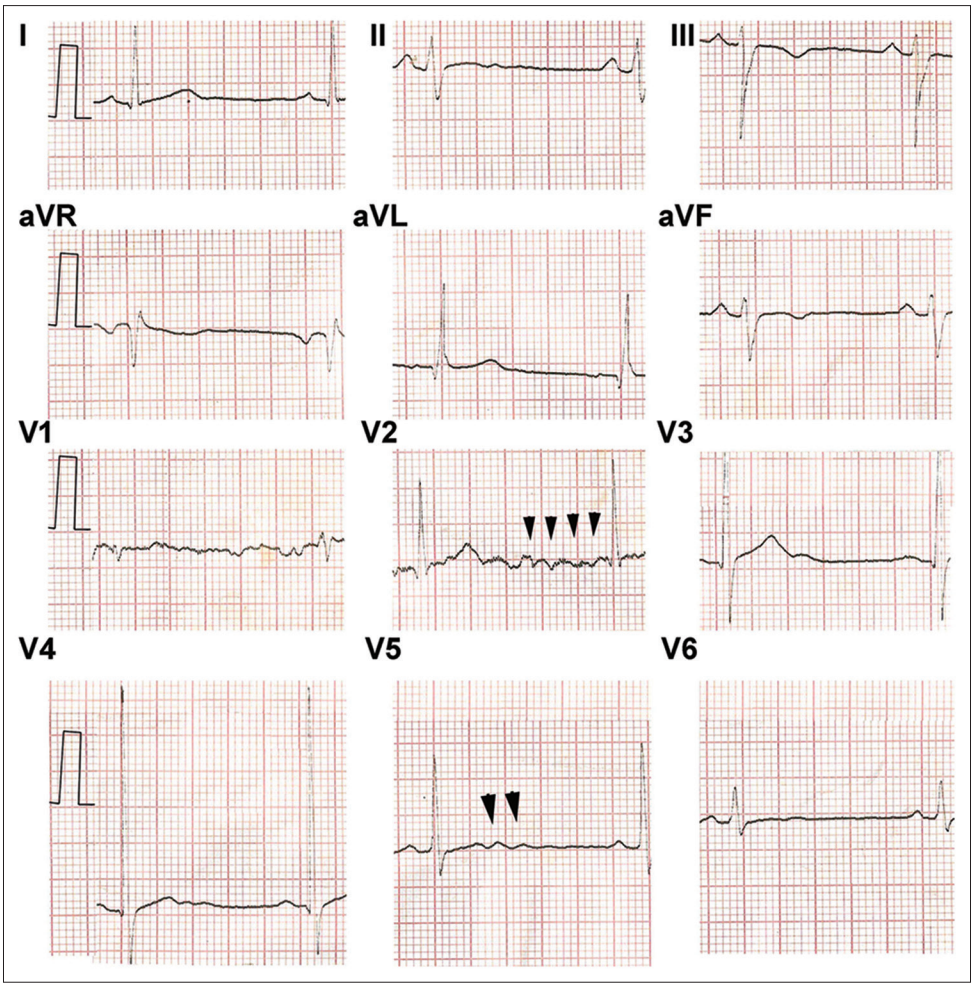

Figure 4: Electrocardiography on admission of patient Case 3 shows bradycardia with ventricular rate of 55 bpm and paroxysmal atrial fibrillation with atrial rate of 500 bpm (arrowheads in V2 and V5). There was T-wave inversion suggestive of myocardial ischemia in contiguous leads of the inferior wall (II, III, aVF)

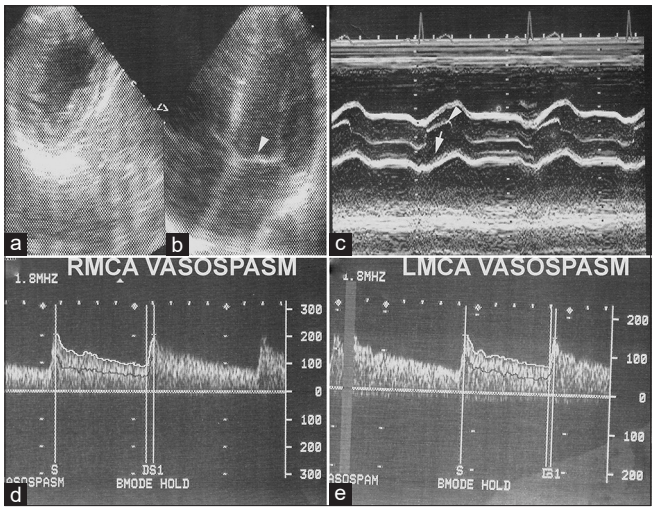

Figure 5: (a-e) The pretreatment two-dimensional echocardiography in short-axis view (a) and long-axis view (b) showing dilated ventricular dimensions suggestive of dilated cardiomyopathy. The M-mode (c) arrow and arrowhead) showing aortic valve vegetations. RMCA: Right middle cerebral artery (d), LMCA: Left middle cerebral artery (e) vaso-spasm.

PE or DVT was not previously present. The therapeutic anticoagulation can stop after 3 months, provided the patient has recovered from COVID-19 and has no ongoing risk factors for thrombosis or other indications for anticoagulation (e.g., prolonged immobilization or atrial fibrillation).

Conclusion

Noninvasive ultrasound imaging modalities in combination with CAT scans provided insightful characterization of the hypercoagulable state of COVID-19 infection, which helped guide therapeutic intervention.

Declaration of patient consent

The authors certify that they have obtained all appropriate patient consent forms. In the form, the patient(s) has/have given his/her/their consent for his/her/their images and other clinical information to be reported in the journal. The patients understand that their names and initials will not be published and due efforts will be made to conceal their identity, but anonymity cannot be guaranteed.

Financial support and sponsorship
Nil.

Conflicts of interest
There are no conflicts of interest.

References

1. Zhou F, Yu T, Du R, Fan G, Liu Y, Liu Z, *et al.* Clinical course and risk factors for mortality of adult inpatients with COVID-19 in Wuhan, China: A retrospective cohort study. Lancet 2020;395:1054-62.
2. Guan, WJ, Ni ZY, Hu Y, Liang WH, Ou CQ, He JX, *et al*. Clinical characteristics of coronavirus disease 2019 in China. N Engl J Med 2020;382:1708-20.
3. Huang C, Wang Y, Li X, Ren L, Zhao J, Hu Y, *et al.* Clinical features of patients infected with 2019 novel coronavirus in Wuhan, China. Lancet 2020;395:497-506.
4. Tang N, Li D, Wang X, Sun Z. Abnormal coagulation parameters are associated with poor prognosis in patients with novel coronavirus pneumonia. J Thromb Haemost 2020;18:844-7.
5. Klok FA, Kruip MJ, van der Meer NJ, Arbous MS, Gommers DA, Kant KM, *et al.* Incidence of thrombotic complications in critically ill ICU patients with COVID-19. Thromb Res 2020;191:145-7.
6. Llitjos JF, Leclerc M, Chochois C, Monsallier JM, Ramakers M, Auvray M, *et al*. High incidence of venous thromboembolic events in anticoagulated severe COVID-19 patients. J Thromb Haemost 2020;18:1743-6.
7. Campbell CM, Kahwash R. Will complement inhibition be the new target in treating COVID-19-related systemic thrombosis? Circulation 2020;141:1739-41.
8. Varga Z, Flammer AJ, Steiger P, Haberecker M, Andermatt R, Zinkernagel AS, *et al*. Endothelial cell infection and endotheliitis in COVID-19. Lancet 2020;395:1417-8.
9. Oudkerk M, Büller HR, Kuijpers D, van Es N, Oudkerk SF, McLoud T, *et al*. Diagnosis, prevention, and treatment of thromboembolic complications in COVID-19: Report of the national institute for public health of the Netherlands. Radiology 2020;297:E216-22.
10. Tang N, Bai H, Chen X, Gong J, Li D, Sun Z. Anticoagulant treatment is associated with decreased mortality in severe coronavirus disease 2019 patients with coagulopathy. J Thromb Haemost 2020;18:1094-9.
11. Han H, Yang L, Liu R, Liu F, Wu KL, Li J, *et al*. Prominent changes in blood coagulation of patients with SARS-CoV-2 infection. Clin Chem Lab Med 2020;58:1116-20.
12. Lodigiani C, Iapichino G, Carenzo L, Cecconi M, Ferrazzi P, Sebastian T, *et al*. Venous and arterial thromboembolic complications in COVID-19 patients admitted to an academic hospital in Milan, Italy. Thromb Res 2020;191:9-14.
13. Wichmann D, Sperhake JP, Lütgehetmann M, Steurer S, Edler C, Heinemann A, *et al*. Autopsy findings and venous thromboembolism in patients with COVID-19: A prospective cohort study. Ann Intern Med 2020;173:268-77.
14. Menter T, Haslbauer JD, Nienhold R, Savic S, Hopfer H, Deigendesch N, *et al*. Postmortem examination of COVID-19 patients reveals diffuse alveolar damage with severe capillary congestion and variegated findings in lungs and other organs suggesting vascular dysfunction. Histopathology 2020;77:198-209.
15. Ackermann M, Verleden SE, Kuehnel M, Haverich A, Welte T, Laenger F, *et al*. Pulmonary vascular endothelialitis, thrombosis, and angiogenesis in COVID-19. N Engl J Med 2020;383:120-8.
16. Landstra CP, de Koning EJ. COVID-19 and diabetes: Understanding the interrelationship and risks for a severe course. Front Endocrinol (Lausanne) 2021;12:649525.
17. Stegenga ME, van der Crabben SN, Blümer RM, Levi M, Meijers JC, Serlie MJ, *et al*. Hyperglycemia enhances coagulation and reduces neutrophil degranulation, whereas hyperinsulinemia inhibits fibrinolysis during human endotoxemia. Blood 2008;112:82-9.
18. Lang RM, Badano LP, Mor-Avi V, Afilalo J, Armstrong A, Ernande L, *et al*. Recommendations for cardiac chamber quantification by echocardiography in adults: An update from the American Society of Echocardiography and the European Association of Cardiovascular Imaging. Eur Heart J Cardiovasc Imaging 2015;16:233-71.
19. Liboni W, Allais G, Mana O, Molinari F, Grippi G, Negri E, *et al.* Transcranial Doppler for monitoring the cerebral blood flow dynamics: Normal ranges in the Italian female population. Panminerva Med 2006;48:187-91.
20. Samagh N, Bhagat H, Jangra K. Monitoring cerebral vasospasm: How much can we rely on transcranial Doppler. J Anaesthesiol Clin Pharmacol 2019;35:12-8.
21. Abou-Ismail MY, Diamond A, Kapoor S, Arafah Y, Nayak L. The hypercoagulable state in COVID-19: Incidence, pathophysiology, and management. Thromb Res 2020;194:101-15.
22. Ciceri F, Beretta L, Scandroglio AM, Colombo S, Landoni G, Ruggeri A, *et al.* Microvascular COVID-19 lung vessels obstructive thromboinflammatory syndrome (MicroCLOTS): An atypical acute respiratory distress syndrome working hypothesis. Crit Care Resusc 2020;22:95-7.
23. Dunn E, Grant P. Type 2 diabetes: an atherothrombotic syndrome. Curr Mol Med 2005;5:323-32.
24. Bode B, Garrett V, Messler J, McFarland R, Crowe J, Booth R, *et al*. Glycemic characteristics and clinical outcomes of COVID-19 patients hospitalized in the United States. J Diabetes Sci Technol 2020;14:813-21.
25. Guo W, Li M, Dong Y, Zhou H, Zhang Z, Tian C, *et al*. Diabetes is a risk factor for the progression and prognosis of COVID-19. Diabetes Metab Res Rev 2020;36:1-9.